SERBIAN JOURNAL OF ELECTRICAL ENGINEERING
Vol. 4, No. 2, November 2007, 119-132

Dynamic Modeling and Simulation of an Induction Motor with Adaptive Backstepping Design of an Input-Output Feedback Linearization Controller in Series Hybrid Electric Vehicle

Mehran Jalalifar[1], Amir Farrokh Payam[2], Seyed Morteza Saghaeian Nezhad[3], Hassan Moghbeli[4]

Abstract: In this paper using Adaptive backstepping approach an adaptive rotor flux observer which provides stator and rotor resistances estimation simultaneously for induction motor used in series hybrid electric vehicle is proposed. The controller of induction motor (IM) is designed based on input-output feedback linearization technique. Combining this controller with adaptive backstepping observer the system is robust against rotor and stator resistances uncertainties. In additional, mechanical components of a hybrid electric vehicle are called from the Advanced Vehicle Simulator Software Library and then linked with the electric motor. Finally, a typical series hybrid electric vehicle is modeled and investigated. Various tests, such as acceleration traversing ramp, and fuel consumption and emission are performed on the proposed model of a series hybrid vehicle. Computer simulation results obtained, confirm the validity and performance of the proposed IM control approach using for series hybrid electric vehicle.

Keywords: Adaptive backstepping observer, Series electric vehicle.

1 Introduction

Nowadays the air pollution and economical issues are the major driving forces in developing electric vehicles (EVs).

In recent years EVs and hybrid electric vehicles (HEVs) are the only alternatives for a clean, efficient and environmentally friendly urban transportation system [1]. HEVs meet both consumer needs as well as car manufacturer needs. They give the consumer the ability to use the car for long periods of time

[1]Islamic Azad University, Fereydan Branch, Esfahan, Iran; Email: mehran_j1356@yahoo.com
[2]Dept. of Electrical & Computer Engineering, University of Tehran, Tehran 11365/4563, Iran;
[3]Dept. of Electrical & Computer Engineering, Isfahan University of Technology, Isfahan, Iran.
[4]Dept. of Electrical & Computer Engineering, Isfahan University of Technology, Isfahan, Iran;
Email :hamoghbeli@yahoo.com

without recharging. HEVs also take a giant step forward in meeting low emission standards set by the Partnership for a New Generation of Vehicles.

Because of simple and rugged construction, low cast and maintenance, high performance and sufficient starting torque and good ability of acceleration, squirrel cage induction motor is a good candidate for EVs [2].

In this paper by using an input-output feedback linearization technique combined with an adaptive backstepping observer in stator reference frame the induction motor [3] using in series hybrid electric vehicle is controlled. One of the best advantages of this control method is eliminating the flux sensor and decreases the cost of controller in addition the control system is robust respect to resistances variations and external load torque.

Advanced vehicle simulator (ADVISOR) provides the vehicle engineering community with an easy-to-use, flexible, yet robust and supported analysis package for advanced vehicle modeling. It is primarily used to quantify fuel economy, the performance, and the emissions of vehicles that use alternative technologies including fuel cells, batteries, electric motors, and ICE in hybrid configurations. But the components in ADVISOR have been modeled simply and only with static model to decrease the simulation time [4].

In this paper using MATLAB/SIMULINK software, dynamic modeling of an induction motor that is used in series hybrid electric vehicle and controlled by input-output feedback linearization method combined with adaptive backstepping observer is investigated and then simulated separately by linking the mechanical components for a series hybrid electric vehicle from the ADVISOR software library. At the end, a typical HEV is modeled and investigated. Simulation results obtained show the IM and other components performances for a typical city drive cycle.

2 The Performance of an Electric Vehicle

The first step in vehicle performance modeling is to write an equation for the electric force. This is the force transmitted to the ground through the drive wheels, and propelling the vehicle forward. This force must overcome the road load and accelerate the vehicle as shown in Fig. 1 [5].

The rolling resistance is primarily due to the friction of the vehicle tires on the road and can be written as:

$$f_{roll} = f_r Mg \,, \tag{1}$$

where M is the vehicle mass, f_r is the rolling resistance coefficient and g is gravity acceleration.

The aerodynamic drag is due to the friction of the body of vehicle moving through the air. The formula for this component is as in the following:

$$f_{AD} = \frac{1}{2}\xi C_D A V^2, \tag{2}$$

where ξ is the air mass density, and V, C_D and A are the speed, the aerodynamic coefficient, and the frontal area of the vehicle, respectively.

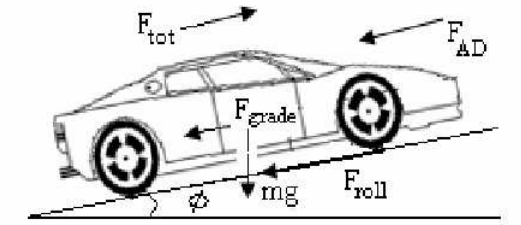

Fig. 1 – *A summary of forces on a vehicle.*

The gravity force due to the slope of the road can be expressed by:

$$f_{grade} = Mg \sin\alpha, \tag{3}$$

where α is the grade angle.

In addition to the forces shown in Fig. 3, another one is needed to provide the linear acceleration of the vehicle given by:

$$f_{acc} = M\alpha = M\frac{\mathrm{d}V}{\mathrm{d}t}. \tag{4}$$

The propulsion system must now overcome the road loads and accelerate the vehicle by the tractive force, F_{tot}, as follows:

$$F_{tot} = f_{roll} + f_{AD} + f_{grade} + f_{acc}. \tag{5}$$

A typical road load characteristic as a function of the speed and mass of a vehicle is shown in Fig. 2.

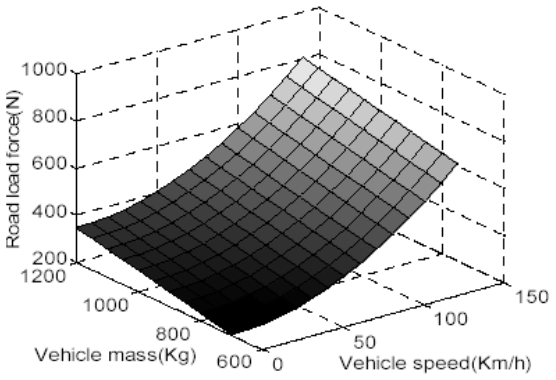

Fig. 2 – *The road profile as a function of speed and mass of a vehicle* ($\alpha = 0°$).

Wheels and axels convert F_{tot} and the speed of vehicle to torque and angular speed requirements for the differential as follow [4]:

$$T_{wheel} = F_{tot} r_{wheel}, \quad \omega_{wheel} = \frac{V}{r_{wheel}}, \tag{6}$$

where T_{wheel}, r_{wheel}, and ω_{wheel} are the tractive torque, the radius, and the angular velocity at the wheels, respectively.

The angular velocity and torque of the wheels are converted to motor rpm and motor torque requirements using the gears ratio at differential and gearbox as follows:

$$\omega_m = G_{fd} G_{gb} \omega_{wheel}, \quad T_m = \frac{T_{wheel}}{G_{fd} G_{gb}}, \tag{7}$$

where G_{fd} and G_{gb} are respectively differential and gear box gears ratios.

A series HEV consists of two major group components as shown in Fig. 3:

- Mechanical components (engine, wheels, axels and transmission box) and
- Electrical components (batteries and electric motor).

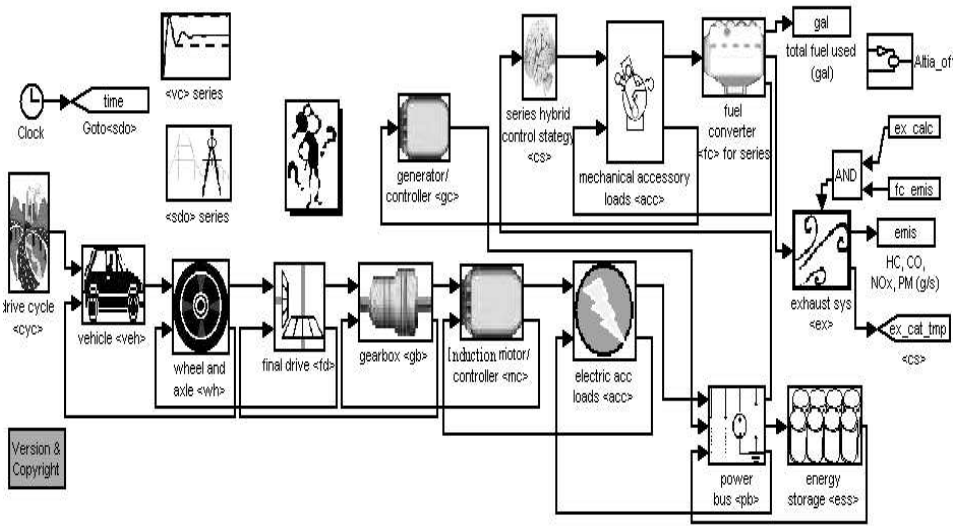

Fig. 3 – *A series hybrid electric vehicle.*

3 Electric Motor

Due to the simple and rugged construction, low cast and maintenance, high performance and sufficient starting torque and good ability of acceleration, squirrel cage induction motor is one of the well suited motors for the electric propulsion systems [6]. In this section first modeling of the induction motor in

stator fixed reference frame and then designing an input-output controller combined with adaptive backstepping observer for IM [3] is investigated.

A. *Input-Output Feedback linearization Controller Design*

The square of rotor flux amplitude is taken as the first output of the controlled system

$$\begin{aligned} y_1 &= \psi_{ra}{}^2 + \psi_{rb}{}^2 = \psi_r{}^2, \\ e_1 &= y_1 - y_{1d} = \psi_r{}^2 - \psi_r^{r2}, \end{aligned} \tag{8}$$

where ψ_r^r is the reference signal for rotor flux amplitude.

Differentiating y_1 so much inputs (u_{sa}, u_{sb}) appear in our equations,

$$\dot{y}_1 = 2\psi_{ra}\left(-\frac{R_r}{L_r}\psi_{ra} + \frac{R_r}{L_r}Mi_{sa}\right) + 2\psi_{rb}\left(-\frac{R_r}{L_r}\psi_{rb} + \frac{R_r}{L_r}Mi_{sb}\right). \tag{9}$$

Then

$$\begin{aligned} \ddot{y}_1 = &-4\frac{R_r}{L_r}\psi_{ra}\left(-\frac{R_r}{L_r}\psi_{ra} + \frac{R_r}{L_r}Mi_{sa}\right) + \\ &+2\frac{R_r}{L_r}M\psi_{ra}\left(\frac{MR_r}{\sigma L_s L_r^2}\psi_{ra} - \frac{M^2R_r + L_r^2R_s}{\sigma L_s L_r^2}i_{sa} + \frac{u_{sa}}{\sigma L_s}\right) - \\ &-4\frac{R_r}{L_r}\psi_{rb}\left(\frac{R_r}{L_r}\psi_{rb} + \frac{R_r}{L_r}Mi_{sb}\right) + 2\frac{R_r}{L_r}M\psi_{rb}. \end{aligned} \tag{10}$$

If e_1 dynamic force to be

$$k_{11}\ddot{e}_1 + k_{12}\dot{e}_1 + k_{13}e_1 = 0,$$

we have

$$\begin{aligned} &k_{11}(\ddot{y}_1 - \ddot{y}_{1d}) + k_{12}(\dot{y}_1 - \dot{y}_{1d}) + k_{13}(y_1 - y_{1d}) = 0, \\ &\ddot{y}_1 = \frac{k_{12}}{k_{11}}(\dot{y}_{1d} - \dot{y}_1) + \frac{k_{13}}{k_{11}}(y_{1d} - y_1) + \ddot{y}_{1d} = \\ &= \frac{k_{13}}{k_{11}}(\psi_r^{r2} - \psi_r^2) - \frac{k_{12}}{k_{11}}\left\{2\psi_{ra}\left(-\frac{R_r}{L_r}\psi_{ra} + \frac{R_r}{L_r}Mi_{sa}\right) + \right. \\ &\left. +2\psi_{rb}\left(-\frac{R_r}{L_r}\psi_{rb} + \frac{R_r}{L_r}Mi_{sb}\right)\right\} - 2\psi_r^r\dot{\psi}_r^r + 2\left(\dot{\psi}_r^{r2} + \psi_r^r\ddot{\psi}_r^r\right). \end{aligned} \tag{11}$$

Now the motor developed electromagnetic torque is considered as the second output

$$y_2 = te = \frac{n_p M}{2L_r}(\psi_{ra} i_{sb} - \psi_{rb} i_{sa})$$
$$e_2 = y_2 - y_{2d} = te - te^r \tag{12}$$

where te^r is the reference signal for developed electromagnetic torque.

Time derivative of y_2 is:

$$\dot{y}_2 = \frac{n_p M}{2L_r}\left\{\psi_{ra}\left(-\frac{n_p M}{\sigma L_s L_r}\omega\psi_{ra} - \frac{M^2 R_r + L_r^2 R_s}{\sigma L_s L_r^2} i_{sb} + \frac{u_{sb}}{\sigma L_s}\right) + \right.$$
$$+ i_{sb}\left(-\frac{R_r}{L_r}\psi_{ra} - n_p\omega\psi_{rb}\right) - \psi_{rb}\left(\frac{n_p M}{\sigma L_s L_r}\omega\psi_{rb} - \frac{M^2 R_r + L_r^2 R_s}{\sigma L_s L_r^2} i_{sa} + \frac{u_{sa}}{\sigma L_s}\right) - \tag{13}$$
$$\left. - i_{sa}\left(-\frac{R_r}{L_r}\psi_{rb} + n_p\omega\psi_{ra}\right)\right\}.$$

By setting e_2 dynamic as

$$k_{21}\dot{e}_2 + k_{22}e_2 = 0,$$

we have

$$k_{21}(\dot{y}_2 - \dot{y}_{2d}) + k_{22}(y_2 - y_{2d}) = 0,$$
$$\dot{y}_2 = \frac{k_{22}}{k_{21}}(y_{2d} - y_2) + \dot{y}_{2d} = \frac{k_{22}}{k_{21}}(te^r - te) + \dot{te}^r. \tag{14}$$

Setting right side of (13) equal to right side of (14), another equation for inputs is achieved

$$\frac{n_p M}{2L_r}\left\{\psi_{ra}\left(-\frac{n_p M}{\sigma L_s L_r}\omega\psi_{ra} - \frac{M^2 R_r + L_r^2 R_s}{\sigma L_s L_r^2} i_{sb} + \frac{u_{sb}}{\sigma L_s}\right) + \right.$$
$$+ i_{sb}\left(-\frac{R_r}{L_r}\psi_{ra} - n_p\omega\psi_{rb}\right) - \psi_{rb}\left(\frac{n_p M}{\sigma L_s L_r}\omega\psi_{rb} - \frac{M^2 R_r + L_r^2 R_s}{\sigma L_s L_r^2} i_{sa} + \frac{u_{sa}}{\sigma L_s}\right) - \tag{15}$$
$$\left. - i_{sa}\left(-\frac{R_r}{L_r}\psi_{rb} + n_p\omega\psi_{ra}\right)\right\} = \frac{k_{22}}{k_{21}}(te^r - te) + \dot{te}^r.$$

Now, from system of two equations, (6 and 10), inputs (u_{sa}, u_{sb}) are found.

To proof the stability of proposed controller, note that according to dynamics of e_1, e_2, if initially $e_1(0) = \dot{e}_1(0) = 0$ and also $e_2(0) = 0$, then $e_1(t), e_2(t) \equiv 0, \ \forall t \geq 0$, perfect tracking is achieved; otherwise, $e_1(t), e_2(t)$ converges to zero exponentially [7].

B. *Adaptive Backstepping Observer Design*

Stator current is measurable and is taken as output:

$$y_a = i_{sa}, y_b = i_{sb}. \tag{16}$$

The prediction model for the backstepping observer is chosen to be

$$\begin{aligned}
p\hat{\psi}_{ra} &= -\frac{\hat{R}_r}{L_r}\hat{\psi}_{ra} - n_p\omega\hat{\psi}_{rb} + \frac{\hat{R}_r}{L_r}My_a,\\
p\hat{\psi}_{rb} &= -\frac{\hat{R}_r}{L_r}\hat{\psi}_{rb} + n_p\omega\hat{\psi}_{ra} + \frac{\hat{R}_r}{L_r}My_b,\\
p\hat{i}_{sa} &= \frac{M\hat{R}_r}{\sigma L_s L_r^2}\hat{\psi}_{ra} + \frac{n_p M}{\sigma L_s L_r}\omega\hat{\psi}_{rb} - \frac{M^2\hat{R}_r + L_r^2\hat{R}_s}{\sigma L_s L_r^2}y_a + \frac{1}{\sigma L_s}u_{sa} + v_a,\\
p\hat{i}_{sb} &= \frac{M\hat{R}_r}{\sigma L_s L_r^2}\hat{\psi}_{rb} - \frac{n_p M}{\sigma L_s L_r}\omega\hat{\psi}_{ra} - \frac{M^2\hat{R}_r + L_r^2\hat{R}_s}{\sigma L_s L_r^2}y_b + \frac{1}{\sigma L_s}u_{sb} + v_b,
\end{aligned} \tag{17}$$

where p is the differential operator and v_a, v_b are the control input to be designed by the backstepping method.

The dynamical equations for the prediction errors are

$$\begin{aligned}
p\tilde{\psi}_{ra} &= -\frac{\tilde{R}_r}{L_r}\psi_{ra} - \frac{\hat{R}_r}{L_r}\tilde{\psi}_{ra} - n_p\omega\tilde{\psi}_{rb} + \frac{\tilde{R}_r}{L_r}My_a,\\
p\tilde{\psi}_{rb} &= -\frac{\tilde{R}_r}{L_r}\psi_{rb} - \frac{\hat{R}_r}{L_r}\tilde{\psi}_{rb} + n_p\omega\tilde{\psi}_{ra} + \frac{\tilde{R}_r}{L_r}My_b,\\
p\tilde{i}_{sa} &= \frac{M\tilde{R}_r}{\sigma L_s L_r^2}\psi_{ra} + \frac{M\hat{R}_r}{\sigma L_s L_r^2}\tilde{\psi}_{ra} + \frac{n_p M}{\sigma L_s L_r}\omega\tilde{\psi}_{rb} - \frac{M^2\tilde{R}_r + L_r^2\tilde{R}_s}{\sigma L_s L_r^2}y_a + v_a,\\
p\tilde{i}_{sb} &= \frac{M\tilde{R}_r}{\sigma L_s L_r^2}\psi_{rb} + \frac{M\hat{R}_r}{\sigma L_s L_r^2}\tilde{\psi}_{rb} - \frac{n_p M}{\sigma L_s L_r}\omega\tilde{\psi}_{ra} - \frac{M^2\tilde{R}_r + L_r^2\tilde{R}_s}{\sigma L_s L_r^2}y_b + v_b,\\
\tilde{y}_a &= \tilde{i}_{sa},\\
\tilde{y}_b &= \tilde{i}_{sb},
\end{aligned} \tag{18}$$

where

$$\begin{aligned}
&\tilde{\psi}_{ra} = \hat{\psi}_{ra} - \psi_{ra}, \tilde{\psi}_{rb} = \hat{\psi}_{rb} - \psi_{rb}, \tilde{i}_{sa} = \hat{i}_{sa} - i_{sa},\\
&\tilde{i}_{sb} = \hat{i}_{sb} - i_{sb}, \quad \tilde{R}_s = \hat{R}_s - R_s, \tilde{R}_r = \hat{R}_r - R_r.
\end{aligned} \tag{19}$$

The first step in the backstepping strategy is to design a stable controller for the integral of the prediction errors $\tilde{y}_a, \tilde{y}_b$ using $\tilde{i}_{sa}, \tilde{i}_{sb}$ as virtual control

variables with stabilizing functions ϕ_a, ϕ_b which is reference for virtual variables. The integral of the prediction errors $\tilde{x}_a, \tilde{x}_b$ are

$$p\tilde{x}_a = \tilde{i}_{sa}, \quad p\tilde{x}_b = \tilde{i}_{sb}. \tag{20}$$

Adding and subtracting ϕ_a, ϕ_b to above equations

$$\begin{aligned} p\tilde{x}_a &= z_a - c_1\tilde{x}_a, \quad p\tilde{x}_b = z_b - c_1\tilde{x}_b, \\ z_a &= \tilde{i}_{sa} - \phi_a, \quad z_b = \tilde{i}_{sb} - \phi_b, \\ \phi_a &= -c_1\tilde{x}_a, \quad \phi_b = -c_1\tilde{x}_b. \end{aligned} \tag{21}$$

The second step in the backstepping strategy is the control of

$$z_a = \tilde{i}_{sa} + c_1\tilde{x}_a, \quad z_b = \tilde{i}_{sb} + c_1\tilde{x}_b. \tag{22}$$

Taking the derivative of z_a and z_b,

$$\begin{aligned} \dot{z}_a &= \frac{M\tilde{R}_r}{\sigma L_s L_r^2}\psi_{ra} + \frac{M\hat{R}_r}{\sigma L_s L_r^2}\tilde{\psi}_{ra} + \frac{n_p M}{\sigma L_s L_r}\omega\tilde{\psi}_{rb} - \frac{M^2\tilde{R}_r + L_r^2\tilde{R}_s}{\sigma L_s L_r^2}y_a + v_a + c_1\tilde{i}_{sa}, \\ \dot{z}_b &= \frac{M\tilde{R}_r}{\sigma L_s L_r^2}\psi_{rb} + \frac{M\hat{R}_r}{\sigma L_s L_r^2}\tilde{\psi}_{rb} - \frac{n_p M}{\sigma L_s L_r}\omega\tilde{\psi}_{ra} - \frac{M^2\tilde{R}_r + L_r^2\tilde{R}_s}{\sigma L_s L_r^2}y_b + v_b + c_1\tilde{i}_{sb} \end{aligned} \tag{23}$$

and selecting following control inputs

$$\begin{aligned} v_a &= -\frac{M\hat{R}_r}{\sigma L_s L_r^2}\tilde{\psi}_{ra} - \frac{n_p M}{\sigma L_s L_r}\omega\tilde{\psi}_{rb} - c_1\tilde{i}_{sa} - c_2 z_a - \tilde{x}_a, \\ v_b &= -\frac{M\hat{R}_r}{\sigma L_s L_r^2}\tilde{\psi}_{rb} + \frac{n_p M}{\sigma L_s L_r}\omega\tilde{\psi}_{ra} - c_1\tilde{i}_{sb} - c_2 z_b - \tilde{x}_b, \end{aligned} \tag{24}$$

yields

$$\begin{aligned} \dot{z}_a &= \frac{M\tilde{R}_r}{\sigma L_s L_r^2}\psi_{ra} - \frac{M^2\tilde{R}_r + L_r^2\tilde{R}_s}{\sigma L_s L_r^2}y_a - c_2 z_a - \tilde{x}_a, \\ \dot{z}_b &= \frac{M\tilde{R}_r}{\sigma L_s L_r^2}\psi_{rb} - \frac{M^2\tilde{R}_r + L_r^2\tilde{R}_s}{\sigma L_s L_r^2}y_b - c_2 z_b - \tilde{x}_b, \end{aligned} \tag{25}$$

where c_1 and c_2 are positive constant design parameters.

Stability analysis of observer is done by the following Lyapunov candidate:

$$V = \frac{1}{2}\left\{\tilde{x}_a^2 + \tilde{x}_b^2 + z_a^2 + z_b^2 + \tilde{\psi}_{ra}^2 + \tilde{\psi}_{rb}^2 + \frac{1}{\gamma_s}\tilde{R}_s^2 + \frac{1}{\gamma_r}\tilde{R}_r^2\right\}. \tag{26}$$

Derivating V along the dynamics of (18, 21 and 25) yields

$$\begin{aligned}\dot{V} = &-c_1\tilde{x}_a^2 - c_1\tilde{x}_b^2 - c_2 z_a^2 - c_2 z_b^2 - \frac{\hat{R}_r}{L_r}\tilde{\psi}_{ra}^2 - \frac{\hat{R}_r}{L_r}\tilde{\psi}_{rb}^2 \\ &+\tilde{R}_s\left\{-\frac{z_a L_r^2}{\sigma L_s L_r^2}y_a - \frac{z_b L_r^2}{\sigma L_s L_r^2}y_b + \frac{1}{\gamma_s}\frac{d\tilde{R}_s}{dt}\right\} \\ +\tilde{R}_r\Bigg\{&\frac{z_a M}{\sigma L_s L_r^2}\psi_{ra} - \frac{M^2 z_a}{\sigma L_s L_r^2}y_a + \frac{z_b M}{\sigma L_s L_r^2}\psi_{rb} - \frac{M^2 z_b}{\sigma L_s L_r^2}y_b - \frac{\tilde{\psi}_{ra}\psi_{ra}}{L_r} \\ &+\frac{M}{L_r}y_a\tilde{\psi}_{ra} - \frac{\tilde{\psi}_{rb}\psi_{rb}}{L_r} + \frac{M}{L_r}y_b\tilde{\psi}_{rb} + \frac{1}{\gamma_r}\frac{d\tilde{R}_r}{dt}\Bigg\}.\end{aligned} \tag{27}$$

By selecting following adaptation laws

$$\begin{aligned}\frac{d\tilde{R}_s}{dt} &= \gamma_s\left\{\frac{z_a L_r^2}{\sigma L_s L_r^2}y_a + \frac{z_b L_r^2}{\sigma L_s L_r^2}y_b\right\} \\ \frac{d\tilde{R}_r}{dt} &= \gamma_r\Bigg\{-\frac{z_a M}{\sigma L_s L_r^2}\psi_{ra} + \frac{M^2 z_a}{\sigma L_s L_r^2}y_a - \frac{z_b M}{\sigma L_s L_r^2}\psi_{rb} + \frac{M^2 z_b}{\sigma L_s L_r^2}y_b \\ &+\frac{\tilde{\psi}_{ra}\psi_{ra}}{L_r} - \frac{M}{L_r}y_a\tilde{\psi}_{ra} + \frac{\tilde{\psi}_{rb}\psi_{rb}}{L_r} - \frac{M}{L_r}y_b\tilde{\psi}_{rb}\Bigg\},\end{aligned} \tag{28}$$

we have $\dot{V} < 0$ outside the equilibrium point

$$(\tilde{x}_a, \tilde{x}_b, z_a, z_b, \tilde{\psi}_{ra}, \tilde{\psi}_{rb}) = (0,0,0,0,0,0).$$

Based on the Barbalat's Lemma, we can obtain $\tilde{x}_a, \tilde{x}_b, z_a, z_b, \tilde{\psi}_{ra}, \tilde{\psi}_{rb}$ will converge to zero as $t \to \infty$. Therefore, the proposed observer is stable, even if parametric uncertainties exist [8]. The block diagram of the proposed controller is given in Fig. 4.

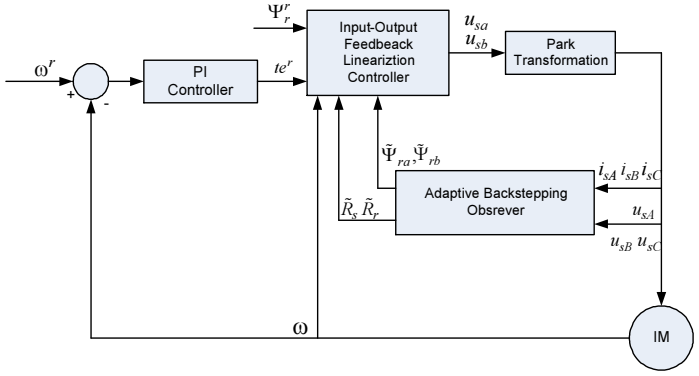

Fig. 4 – *Block diagram of proposed controller.*

4 Battery Modeling

The battery considered in this paper is of the NiMH type for which a simple model is assumed. Therefore, a simplified version of the complex battery model reported in [9] is used.

5 Simulation Results

Simulation results presented in this section, focus on the dynamic behavior of IM and the battery of the vehicle. First the system is simulated for ECE+EUDC test cycle. This cycle is used for emission certification of light duty vehicles in Europe. Due to the electric motor has been modeled dynamically in SIMULINK. The data for IM and EV is in the appendix.

Fig. 5 shows the simulation block diagram.

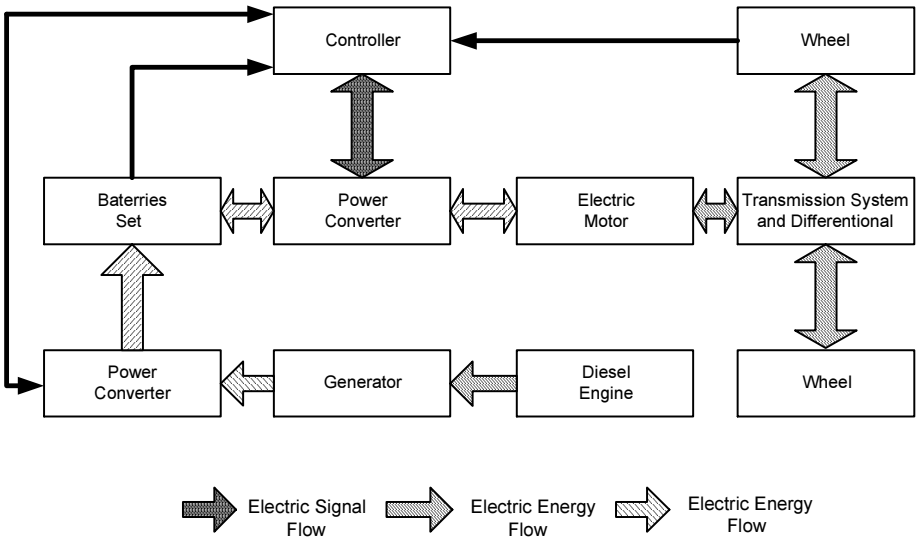

Fig. 5 – *Simulation block diagram*.

The drive cycle gives the required vehicle speed then the torque and speed requested from the electric motor. The current drawn from IM power supply shows the battery performance. The dynamic behavior of the IM in the ECE+EUDC drive cycle is shown in Figs. 6(a) and 6(d). Fig. 6(a) shows the ECE drive cycle. Figs. 6(c) and 6(d) show the IM torque and average torque.

Finally, the system is simulated for fuel consumption and emissions test. The results obtained are shown in Fig. 7 and Fig. 8. Fig. 7 shows the fuel consumption and emissions of diesel engine when the motor is hot at the start of test, and Fig. 8 shows the results when the engine is cool at the start of test. It is

obvious that when the engine is cool, fuel consumption and emissions is increases respect to the engine is hot.

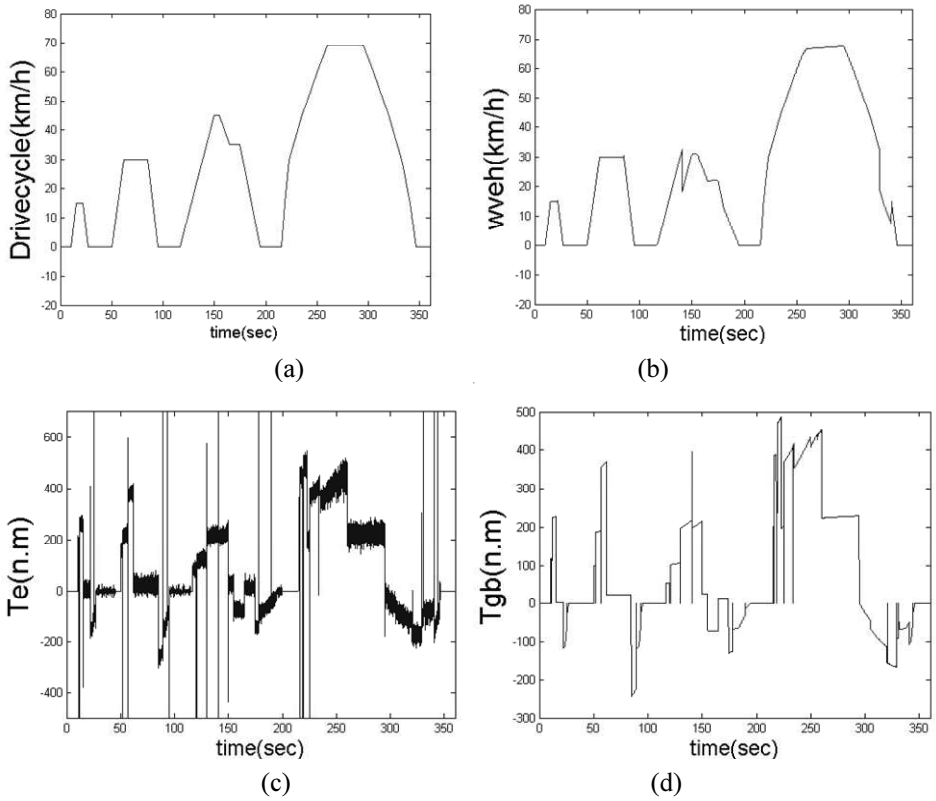

Fig. 6 – (a) ECE *drive cycle*, (b) *Vehicle speed,* (c) *Average torque,* (d) *IM torque.*

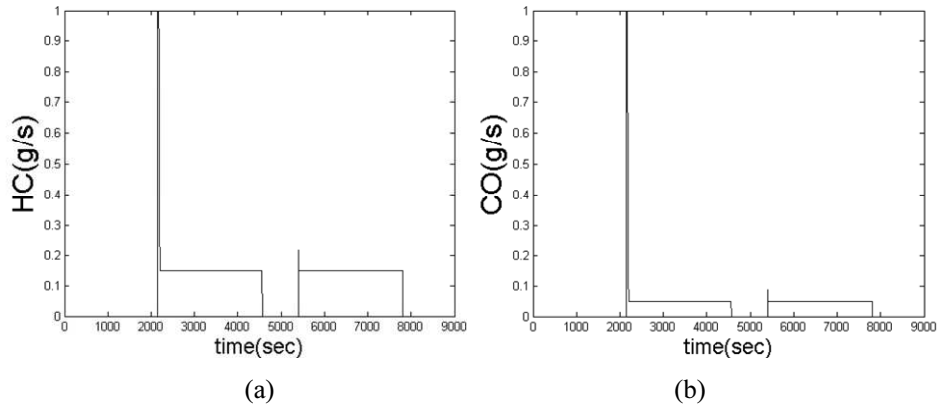

Fig. 7 – (a) HC, (b) CO *consumption.*

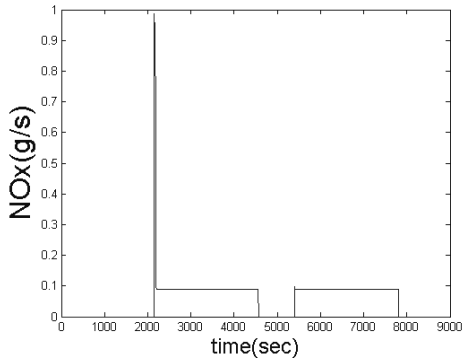

(c)

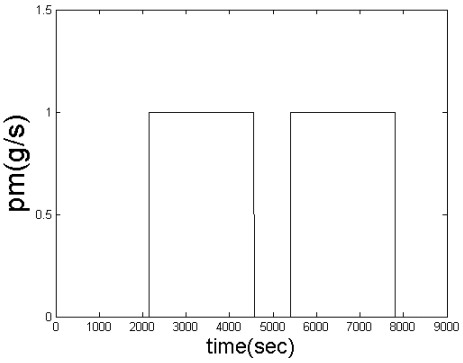

(d)

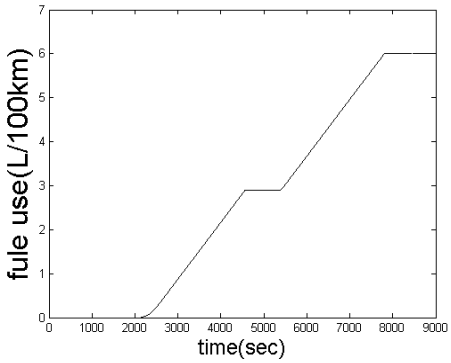

(e)

Fig. 7 – (c) NOX, (d) PM, (e) *Fuel consumption.*

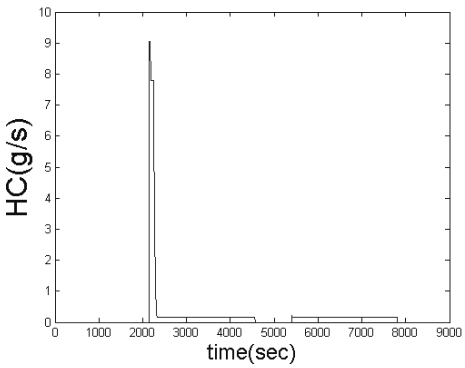

(a)

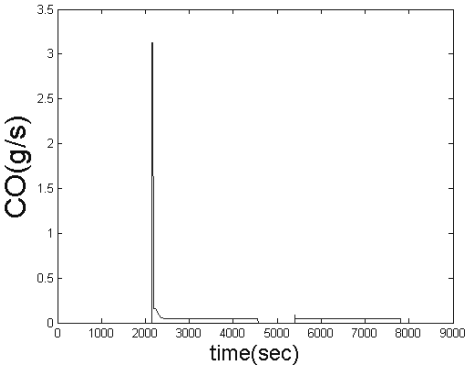

(b)

Fig. 8 – (a) HC, (b) CO *consumption.*

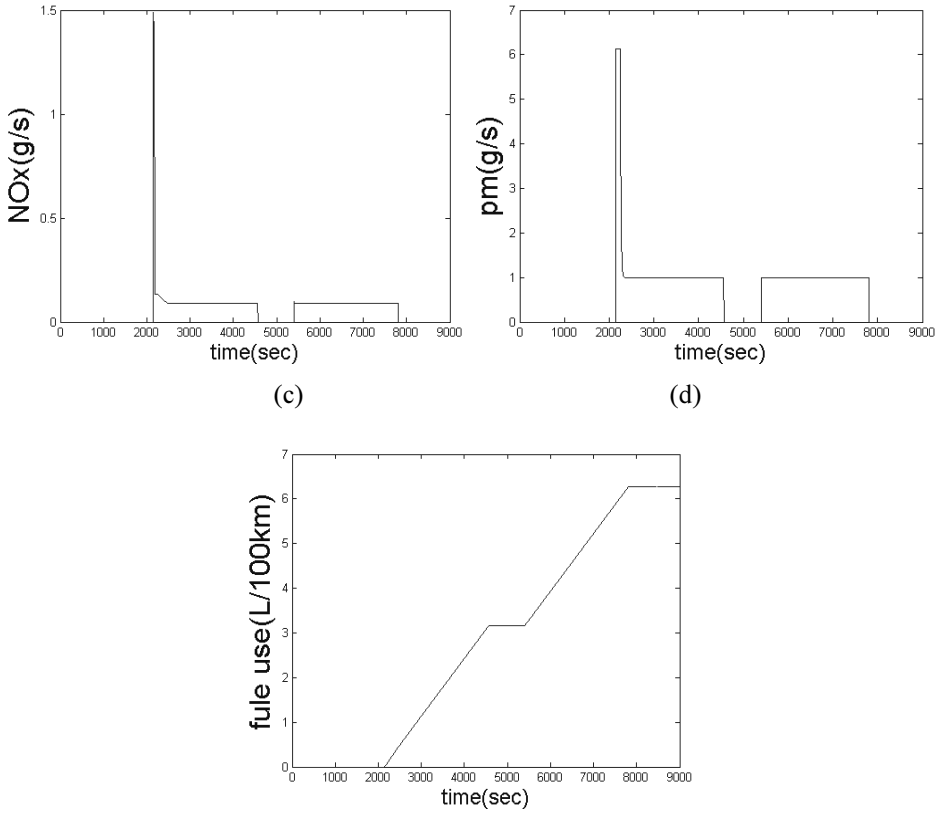

Fig. 8 – (a) HC, (b) CO, (c) NOX, (d) PM, (e) *Fuel consumption.*

6 Conclusion

Steady-state simulation tools such as ADVISOR have been developed in recent years for the design and analysis of electric and hybrid electric vehicles. In the past, dynamic simulation models have focused mainly on the analysis of control strategies. In this paper, the dynamic behavior of the electric motors with input-output state feedback controller combined with adaptive backstepping observer and batteries of a typical series hybrid EV is investigated and simulated by Matlab/Simulink, has been presented and the performance and ability of control strategy is investigated. Simulation results have also been shown the IM dynamic behavior and batteries for various tests such as ECE+EUDC drive cycle, maximum speed, traversing ramp and fuel consumption and emissions.

7 Appendix

A. EV *Data:*

Vehicle total mass of 8200 kg; Air drag coefficient of 0.79; Rolling resistance coefficient of 0.008; Wheel radius of 0.41 m; Level ground; Zero head wind.

B. The IM Parameters:

P_n	$75\,[\mathrm{kW}]$	X_m	$1.95\,[\Omega]$
$P_{\max}$	$189\,[\mathrm{kW}]$	X_{ls}	$0.06\,[\Omega]$
f	$60\,[\mathrm{Hz}]$	X'_{lr}	$0.06\,[\Omega]$
T_n	$209\,[\mathrm{Nm}]$	n_s	$3600\,[\mathrm{r.p.m}]$
$T_{\max}$	$520\,[\mathrm{Nm}]$	J	$1.2\,[\mathrm{kgm}^2]$
R_s	$0.02\,[\Omega]$	P	2
R'_r	$0.01\,[\Omega]$		

8 References

[1] M. Ehsani, K.M. Rahman, H.A. Toliyat: Propulsion System Design of Electric and Hybrid Vehicle, IEEE Tran. On industrial Electronics, Vol. 44, No.1, February 1997.

[2] http://www.ott.doe.gov/hev/

[3] R. Yazdanpanah, A. Farrokh Payam: Direct Torque Control of An Induction Motor Drive Based on Input-Output Feedback Linearization Using Adaptive Backstepping Flux Observer, Proc. 2006 AIESP Conf., Madeira, Portugal.

[4] T. Markel, A. Brooker, T. Hendricks, V. Johnson, K. Kelly, B. Kramer, M. O' Keefe, S. Sprik, K. Wipke: ADVISOR: A Systems Analysis Tool for Advanced Vehicle Modeling, ELSEVIER Journal of Power Sources 110, (2002), pp. 255-266.

[5] Electric Vehicle Technology Explained , Editted by James Larminie, and John Lowry, John Wiley, England, 2003.

[6] A. Rahide: Vector Control of Induction Motor Using Neural Network in Electric Vehicle, Scientific Report, IUST, 2000.

[7] R. Marino, S. Peresada, P. Valigi: Adaptive Input-Output Linearization Control of Induction Motors, IEEE Trans. Automatic Cont., Vol. 38, No. 2, pp. 208-220, Feb. 1993.

[8] Applied Nonlinear Control , Editted by J. E. Slotine, Prentice-Hall International Inc.

[9] S. Sadeghi, J. Milimonfared, M. Mirsalim, M. Jalalifar: Dynamic Modeling and Simulation of a Switched Reluctance Motor in Electric Vehicle, in Proc., 2006 ICIEA Conf.